

Numerical solution of stiff ODEs describing complex homogeneous chemical processes

V.N. Shulyk, O.V. Klymenko, and I.B. Svir*

*Mathematical and Computer Modelling Laboratory, Kharkov National University
of Radioelectronics, 14 Lenin Avenue, Kharkov 61166, Ukraine
E-mail: irina.svir@kture.kharkov.ua*

Received 4 August 2006; accepted September 15 2006

In this manuscript, the two novel numerical methods for stiff ODEs—the Almost Runge–Kutta (ARK) and Aluffi–Pentini (AP)—are applied to the solution of two large stiff ODE systems that model the Belousov–Zhabotinskii reaction and air pollution process. The efficiency and accuracy of the two methods are compared revealing advantages of the ARK method especially for multidimensional ODE systems.

KEY WORDS: stiff ODEs, almost Runge–Kutta method, Aluffi–Pentini method, homogeneous chemical reactions

1. Introduction

A chemical reaction is called homogeneous if all reacting species are uniformly distributed within the reacting mixture. This implies that concentrations of reagents and products depend solely on time and therefore they can be modelled by an ODE system comprising rate laws for individual species. The rate of change of the concentration of each species does not depend explicitly on time, so that the ODE system is autonomous [1]:

$$\mathbf{y}' = \mathbf{f}(\mathbf{y}), \quad 0 \leq t \leq T < \infty \quad \mathbf{y}(0) = \mathbf{y}^0, \quad (1)$$

where T is the reaction (observation) duration and \mathbf{y}^0 the vector of initial species' concentrations.

Chemical reaction mechanisms often include individual steps with very different reaction rates. Mathematically this means that the corresponding ODEs are likely to be stiff since then different components of the system have dramatically different time constants. Moreover, ODE systems modelling complex reactions are often non-linear and cannot be resolved analytically which necessitates their numerical resolution. Since stiff ODEs cannot be solved using classical

*Corresponding author.

methods such as explicit Euler, Runge–Kutta or multistep methods [2–6] special methods are required.

Here we consider two novel one-step numerical methods for stiff ODEs. These are the Almost Runge-Kutta (ARK) method developed by Butcher and Rattenbury [7] and the Aluffi-Pentini (AP) method (as we denote it here for the sake of conciseness) suggested by Aluffi-Pentini et al. [8].

The ARK method is similar to classical Runge–Kutta methods [9] but differs from them in that the former provides (and utilises) approximations of the first and second derivatives of the solution.

The AP method belongs to the class of matrix exponential methods and is based on the idea of iteratively obtaining “exact” solutions to linearised ODEs while avoiding the matrix inversion operation.

Both of these methods may be applied to stiff problems and the aim of this article is to compare their performance properties.

2. Methods for stiff ODEs

Thorough description of the ARK and AP methods is given in [7, 8, 10] so here we give a short account of the methods.

2.1. Almost Runge–Kutta method

In this method, approximations of the solution and its first and second derivatives are evaluated at each step [7]: $\mathbf{y}_1^{[n]} \approx \mathbf{y}(t_n)$; $\mathbf{y}_2^{[n]} \approx h\mathbf{y}'(t_n)$; $\mathbf{y}_3^{[n]} \approx h^2\mathbf{y}''(t_n)$. Every integration step is performed in s stages. Here we consider the three stage implicit ARK method. Approximations to $\mathbf{y}(t_n + hc_i)$ are computed using the formula:

$$\mathbf{Y}_i = \sum_{j=1}^i a_{ij}h\mathbf{F}_j + \sum_{j=1}^3 u_{ij}\mathbf{y}_j^{[n]}, \quad i = 1, 2, 3. \tag{2}$$

The approximations of the solution and its derivatives at the end of the step are given by:

$$\mathbf{y}_i^{[n+1]} = \sum_{j=1}^3 b_{ij}h\mathbf{F}_j + \sum_{j=1}^3 v_{ij}\mathbf{y}_j^{[n]}, \quad i = 1, 2, 3, \tag{3}$$

where the coefficients a_{ij} , u_{ij} and b_{ij} , v_{ij} are elements of the following matrix:

$$\left[\begin{array}{c|ccc} \mathbf{A} & \mathbf{U} \\ \hline \mathbf{B} & \mathbf{V} \end{array} \right] = \left[\begin{array}{ccc|ccc} \frac{2}{5} & 0 & 0 & 1 & \frac{4}{15} & -\frac{2}{45} \\ -\frac{11}{144} & \frac{2}{5} & 0 & 1 & \frac{127}{720} & -\frac{13}{540} \\ -\frac{21}{20} & \frac{8}{5} & \frac{2}{5} & 1 & \frac{1}{20} & 0 \\ \hline -\frac{21}{20} & \frac{8}{5} & \frac{2}{5} & 1 & \frac{1}{20} & 0 \\ 0 & 0 & 1 & 0 & 0 & 0 \\ \frac{39}{20} & -\frac{18}{5} & \frac{3}{2} & 0 & \frac{3}{20} & 0 \end{array} \right], \quad (4)$$

$\mathbf{F}_j = \mathbf{f}(t_n + hc_j, \mathbf{Y}_j)$, $i = 1, 2, 3$; c_j is an element of the three-dimensional vector $\mathbf{c} = \left[\frac{2}{3} \ \frac{1}{2} \ 1 \right]^T$.

2.2. The Aluffi-Pentini method

This method was proposed by Aluffi-Pentini et al. [8] for the solution of stiff ODEs arising in chemical kinetics. At each step of the method the ODE system (1) is linearised as

$$\frac{d\mathbf{y}(t)}{dt} = \mathbf{f}_k + \mathbf{J}_k (\mathbf{y}(t) - \mathbf{y}_k). \quad (5)$$

The exact solution of the latter is given by

$$\mathbf{y}(t) = \mathbf{J}^{-1} (e^{(t-t_k)\mathbf{J}} - \mathbf{I}) \cdot \mathbf{f}_k + \mathbf{y}_k. \quad (6)$$

Letting

$$\boldsymbol{\xi}_k(h) = \mathbf{y}(t) - \mathbf{y}_k, \quad (7)$$

where $h = t - t_k$ one can rewrite the linearised equation (5) in the form

$$\frac{d\boldsymbol{\xi}}{dh} = \mathbf{J}\boldsymbol{\xi} + \mathbf{f}. \quad (8)$$

For a non-singular matrix \mathbf{J} the solution of this ODE is:

$$\boldsymbol{\xi}(h) = \mathbf{J}^{-1} (e^{h\mathbf{J}} - \mathbf{I})\mathbf{f}. \quad (9)$$

Next, the following augmented $(n+1) \times (n+1)$ matrix and $(n+1)$ -dimensional vector are defined as:

$$\mathbf{A} \equiv \begin{pmatrix} \mathbf{J} & \mathbf{f} \\ \mathbf{0}^T & 0 \end{pmatrix}, \quad \boldsymbol{\eta} \equiv \begin{pmatrix} \boldsymbol{\xi} \\ 1 \end{pmatrix}.$$

Using these notations the ODE (8) may be cast into the following homogeneous differential equation

$$\frac{d\eta}{dh} = A\eta, \quad (10)$$

with initial condition $\eta_0 \equiv \begin{pmatrix} 0 \\ 1 \end{pmatrix}$.

The latter ODE allows for the exact solution to be readily obtained:

$$\eta(h) = e^{hA}\eta_0, \quad (11)$$

which requires the evaluation of matrix exponential. This may be efficiently done using by successive matrix squaring with subsequent round-off error smearing as described in the original paper [8].

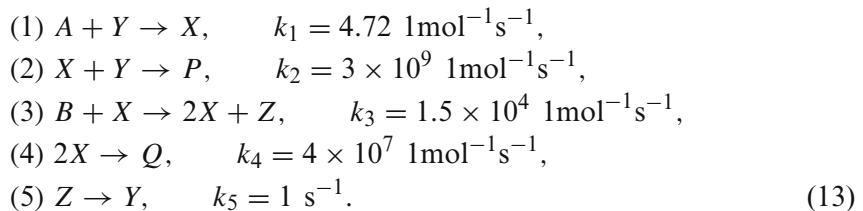
It is clear that η is given by the last column of e^{hA} and the sought solution vector ξ is given by the first n elements of η . Hence, the approximate solution at the step $(k + 1)$ by the AP method is

$$y_{k+1} = y_k + \xi_k(h). \quad (12)$$

3. Numerical solution of stiff ODE systems

3.1. Belousov–Zhabotinskii reaction

The Belousov–Zhabotinskii reaction [11] may be represented by the following scheme of homogeneous chemical reactions:



Letters A, \dots, Z denote species taking part in the reactions. Since the Belousov–Zhabotinskii reaction is homogeneous (meaning that all species are uniformly distributed in the reaction space) we only need to consider variations of the concentrations in time. Each reaction step is characterised by its reaction rate constant. Obviously, the rate constants differ by several orders of magnitude which indicates the likeliness of the corresponding ODE system being stiff.

The initial conditions are given by initial concentrations of species at $t = 0$:

$$A = B = 0.066, \quad Y = X = P = Q = 0, \quad Z = 0.002. \quad (14)$$

The ODE system modelling the reaction scheme (13) was obtained using the algorithm described in [1]:

$$\begin{aligned}
 \frac{dA}{dt} &= -k_1AY, \\
 \frac{dY}{dt} &= -k_1AY - k_2XY + k_5Z, \\
 \frac{dX}{dt} &= -k_2XY + k_3XB - 2k_4X^2 + k_1AY, \\
 \frac{dP}{dt} &= k_2XY, \\
 \frac{dB}{dt} &= -k_3BX, \\
 \frac{dZ}{dt} &= k_3BX - k_5Z, \\
 \frac{dQ}{dt} &= k_4X^2.
 \end{aligned} \tag{15}$$

The latter was considered at the interval $t \in [0, 40]$ and solved using both the ARK and AP methods.

In order to reduce the computational time an algorithm for adaptive step selection was implemented. This is based on “double calculation” when the solution is computed using the step sizes h_k and $2h_k$ which permits to estimate local error, r_k , and then compute the optimal length of the next step using the predefined tolerance, ε [12]:

$$h_{k+1} = h_k(\varepsilon/r_k)^{1/p+1}. \tag{16}$$

It was found during the numerical solution of (15) by the ARK method that some components of the solution become negative when the tolerance is $\varepsilon = 10^{-7}$ or higher (see figure 1). This contradicts the physical meaning of concentrations. However, according to the theorem proved in [2] there always exists a limit of local error ε_0 such that for any $\varepsilon < \varepsilon_0$ the numerical solution of the ODE system (1), which models a chemical process, obtained using the Euler method will remain strictly positive and bounded above for any $t > 0$. The statement of the theorem has been shown to be valid for higher order one-step numerical methods. Hence, it was found that the application of the ARK method with $\varepsilon = 10^{-8}$ gives non-negative solutions. This is exemplified in figure 1 which shows the concentration of Z computed with $\varepsilon = 10^{-7}$ as well as the converged solution. It can be seen that due to the concentration of Z becoming negative at around 12s the rapid increase in it occurs almost two seconds earlier than in the converged solution.

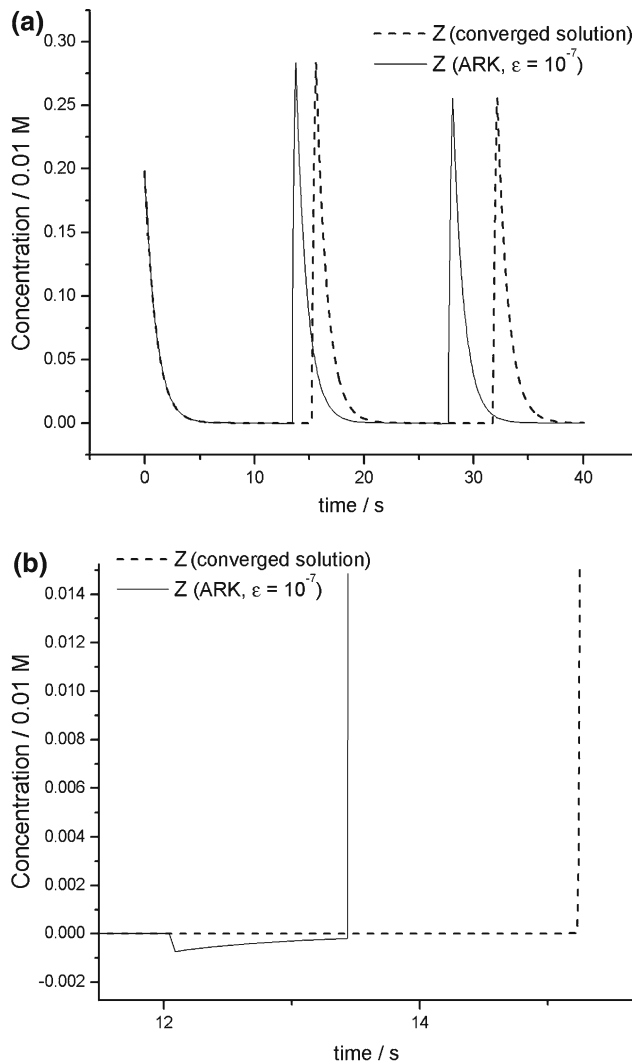


Figure 1. Concentration of Z computed using the ARK method.

The results obtained using the AP method with $\epsilon = 10^{-7}$ are shown in figure 2(a). Despite the absence of negative concentration values the solution strongly deviates from the converged one shown in figure 2(b).

In order to determine the maximum relative error, δ , in the numerically computed concentrations depending on the simulation tolerance the converged solution was computed using the KinFitSim program [13] employing Gear's method with the tolerance $\epsilon = 10^{-14}$.

Figure 3 shows the dependence of the relative error on the tolerance of the method for the ARK and AP methods. For all values of ϵ the relative error is smaller for the ARK method.

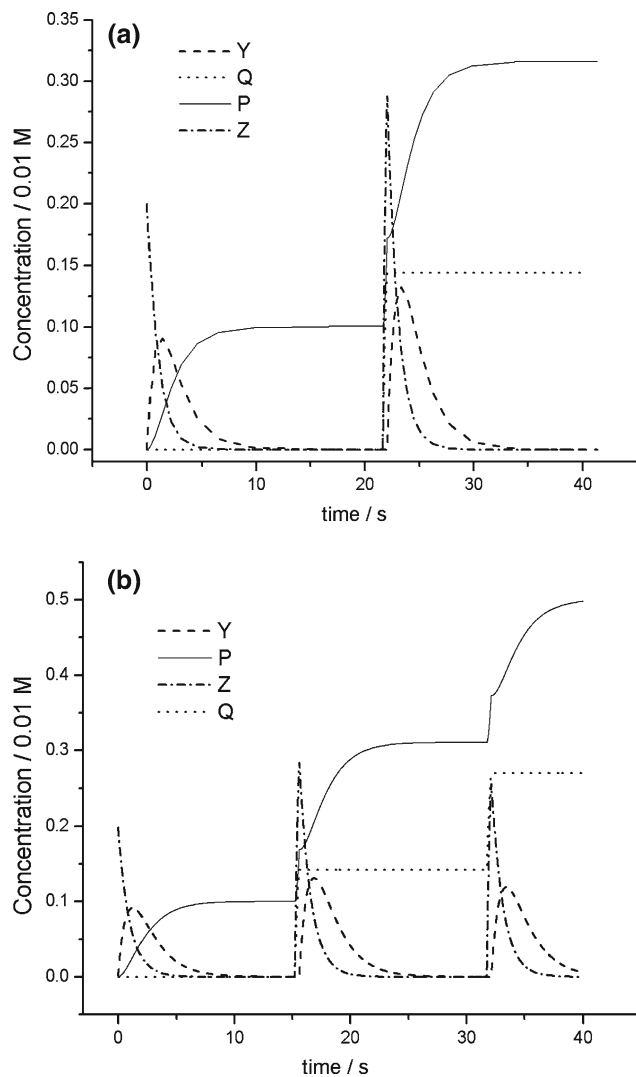


Figure 2. Concentration distributions of species taking part in the Belousov–Zhabotinskii reaction (a) computed using the AP method with $\varepsilon = 10^{-7}$, and (b) converged solution.

Table 1 presents the CPU times and numbers of steps required for each of the two methods to solve the ODE system (15) with $\varepsilon = 10^{-8}$ (all calculations were performed on a PC equipped with Intel Pentium III processor at 800 MHz and 256 MB of RAM). The AP method requires a significantly smaller number of steps than the ARK method. However, computational costs of the two methods (reflected by CPU times) are comparable because the AP method performs more arithmetic operations per step than the ARK method due to the numerical computation of matrix exponential [10].

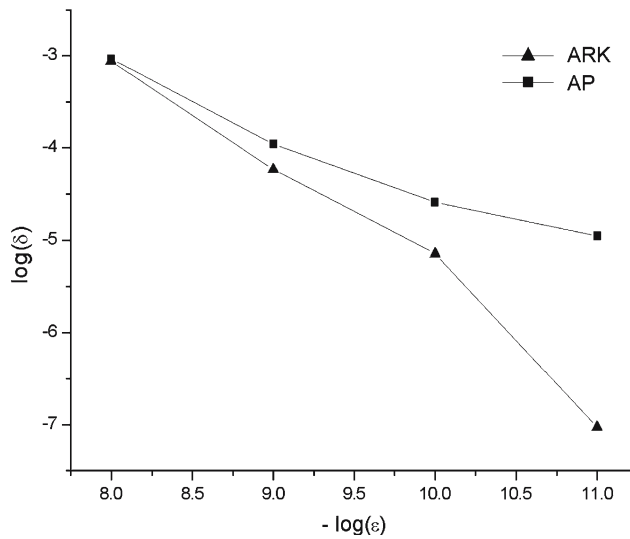


Figure 3. Log–log plot of maximum relative error in computed concentrations as a function of tolerance for the ARK and AP methods (Belousov–Zhabotinskii problem).

Table 1

Computation times and numbers of steps taken by the ARK and AP methods required to solve the ODE system (15) with $\epsilon = 10^{-8}$.

Method	CPU time, s.	Number of steps taken	Number of rejected steps
ARK	9.459	91,073	41
AP	9.353	2872	76

3.2. Pollution problem

The ARK and AP methods were also used to solve a problem from the “Test Set for Initial Value Problem Solvers” [14]. This IVP is a part of the model of air pollution developed at The Dutch National Institute of Public Health and Environmental Protection (RIVM) and it was described by Verwer [15]. The reaction scheme consisting of 25 individual reaction steps and involving 20 different species is given in table 2 along with the corresponding reaction rates, r_j , and rate constants, k_j . The quantities $y_i, i = 1, 20$ denote the concentrations of reacting species: $y_1 = [NO_2], y_2 = [NO], y_3 = [O_3P], y_4 = [O_3], y_5 = [HO_2], y_6 = [OH], y_7 = [HCHO], y_8 = [CO], y_9 = [ALD], y_{10} = [MEO_2], y_{11} = [C_2O_3], y_{12} = [CO_2], y_{13} = [PAN], y_{14} = [CH_3O], y_{15} = [HNO_3], y_{16} = [O1D], y_{17} = [SO_2], y_{18} = [SO_4], y_{19} = [NO_3], y_{20} = [N_2O_5]$.

The mathematical model of the reaction scheme in Table 2 is the following system of ordinary differential reactions:

$$\frac{dy}{dt} = \mathbf{f}(\mathbf{y}), \quad \mathbf{y} \in R^{20}, \quad 0 \leq t \leq 60, \tag{17}$$

where the right-hand side vector-function is defined in (18).

$$\mathbf{f}(\mathbf{y}) = \begin{pmatrix} -\sum_{j \in \{1,10,14,23,24\}} r_j + \sum_{j \in \{2,3,9,11,12,22,25\}} r_j \\ -r_2 - r_3 - r_9 - r_{12} + r_1 + r_{21} \\ -r_{15} + r_1 + r_{17} + r_{19} + r_{22} \\ -r_2 - r_{16} - r_{17} - r_{23} + r_{15} \\ -r_3 + 2r_4 + r_6 + r_7 + r_{13} + r_{20} \\ -r_6 - r_8 - r_{14} - r_{20} + r_3 + 2r_{18} \\ -r_4 - r_5 - r_6 + r_{13} \\ r_4 + r_5 + r_6 + r_7 \\ -r_7 - r_8 \\ -r_{12} + r_7 + r_9 \\ -r_9 - r_{10} + r_8 + r_{11} \\ r_9 \\ -r_{11} + r_{10} \\ -r_{13} + r_{12} \\ r_{14} \\ -r_{18} - r_{19} + r_{16} \\ -r_{20} \\ r_{20} \\ -r_{21} - r_{22} - r_{24} + r_{23} + r_{25} \\ -r_{25} + r_{24} \end{pmatrix}. \tag{18}$$

The initial concentrations are given by the vector

$$y_0 = (0 \ 0.2 \ 0 \ 0.04 \ 0 \ 0 \ 0.1 \ 0.3 \ 0.01 \ 0 \ 0 \ 0 \ 0 \ 0 \ 0 \ 0 \ 0.007 \ 0 \ 0 \ 0)^T.$$

For the solution of the ODE system (17) the algorithm of adaptive step size selection based on “double calculation” and expression (16) were also employed.

The numerical solution obtained using the AP method with tolerance $\varepsilon = 10^{-6}$ reveals that the concentration of NO₃ species (y_{19}) gets negative values at some time points and displays non-physical oscillations (Figure (4a)). The numerical solution obtained using the ARK method with the same tolerance is also invalid because of irregular oscillations despite the fact that all concentration values are non-negative. The converged solution for the same species is attained with tolerance $\varepsilon = 10^{-8}$ for both methods and it is shown in figure 5.

The reference data provided in the Test Set for IVP Solvers [14] for the problem at hand in the form of concentration values at the end of the integration interval have allowed us to investigate the convergence of the numerical results.

Table 2
Reaction scheme of the air pollution process.

No.	Reaction	Reaction rate	Rate constant
1	$NO_2 \rightarrow NO + O_3P$	$r_1 = k_1 y_1$	$k_1 = 0.35$
2	$NO + O_3 \rightarrow NO_2$	$r_2 = k_2 y_2 y_4$	$k_2 = 26.6$
3	$HO_2 + NO \rightarrow NO_2 + OH$	$r_3 = k_3 y_5 y_2$	$k_3 = 0.123 \times 10^5$
4	$HCHO \rightarrow 2HO_2 + CO$	$r_4 = k_4 y_7$	$k_4 = 0.860 \times 10^{-3}$
5	$HCHO + OH \rightarrow HO_2 + CO$	$r_5 = k_5 y_7 y_6$	$k_5 = 0.150 \times 10^5$
6	$HCHO \rightarrow CO$	$r_6 = k_6 y_7$	$k_6 = 0.820 \times 10^{-3}$
7	$ALD \rightarrow MEO_2 + HO_2 + CO$	$r_7 = k_7 y_9$	$k_7 = 0.130 \times 10^{-3}$
8	$ALD + OH \rightarrow C_2O_3$	$r_8 = k_8 y_9 y_6$	$k_8 = 0.240 \times 10^5$
9	$C_2O_3 + NO \rightarrow NO_2 + MEO_2 + CO_2$	$r_9 = k_9 y_{11} y_2$	$k_9 = 0.165 \times 10^5$
10	$C_2O_3 + NO_2 \rightarrow PAN$	$r_{10} = k_{10} y_{11} y_1$	$k_{10} = 0.900 \times 10^4$
11	$PAN \rightarrow C_2O_3 + NO_2$	$r_{11} = k_{11} y_{13}$	$k_{11} = 0.022$
12	$MEO_2 + NO \rightarrow CH_3O + NO_2$	$r_{12} = k_{12} y_{10} y_2$	$k_{12} = 0.120 \times 10^5$
13	$CH_3O \rightarrow HCHO + HO_2$	$r_{13} = k_{13} y_{14}$	$k_{13} = 1.88$
14	$NO_2 + OH \rightarrow HNO_3$	$r_{14} = k_{14} y_1 y_6$	$k_{14} = 0.163 \times 10^5$
15	$O_3P \rightarrow O_3$	$r_{15} = k_{15} y_3$	$k_{15} = 0.480 \times 10^7$
16	$O_3 \rightarrow O_1D$	$r_{16} = k_{16} y_4$	$k_{16} = 0.350 \times 10^{-3}$
17	$O_3 \rightarrow O_3P$	$r_{17} = k_{17} y_4$	$k_{17} = 0.0175$
18	$O_1D \rightarrow 2OH$	$r_{18} = k_{18} y_{16}$	$k_{18} = 0.100 \times 10^9$
19	$O_1D \rightarrow O_3P$	$r_{19} = k_{19} y_{16}$	$k_{19} = 0.444 \times 10^{12}$
20	$SO_2 + OH \rightarrow SO_4 + HO_2$	$r_{20} = k_{20} y_{17} y_6$	$k_{20} = 0.124 \times 10^4$
21	$NO_3 \rightarrow NO$	$r_{21} = k_{21} y_{19}$	$k_{21} = 2.10$
22	$NO_3 \rightarrow NO_2 + O_3P$	$r_{22} = k_{22} y_{19}$	$k_{22} = 5.78$
23	$NO_2 + O_3 \rightarrow NO_3$	$r_{23} = k_{23} y_1 y_4$	$k_{23} = 0.0474$
24	$NO_3 + NO_2 \rightarrow N_2O_5$	$r_{24} = k_{24} y_{19} y_1$	$k_{24} = 0.178 \times 10^4$
25	$N_2O_5 \rightarrow NO_3 + NO_2$	$r_{25} = k_{25} y_{20}$	$k_{25} = 3.12$

Table 3

Computation times and numbers of steps taken by the ARK and AP methods required to solve the ODE systems (17) – (18) with $\varepsilon = 10^{-8}$.

Method	CPU time, s.	Number of steps taken	Number of rejected steps
ARK	71.71	33,487	0
AP	430.56	2636	698

The dependence of the maximum relative error on the tolerance is demonstrated in figure 6. As in the case of the Belousov–Zhabotinskii problem, the relative error is smaller for the ARK method for all values of ε . Moreover, the difference becomes more pronounced for lower values of ε (higher accuracy).

The CPU times and numbers of integration steps are given in table 3 along with the numbers of rejected steps. These values correspond to the tolerance $\varepsilon = 10^{-8}$.

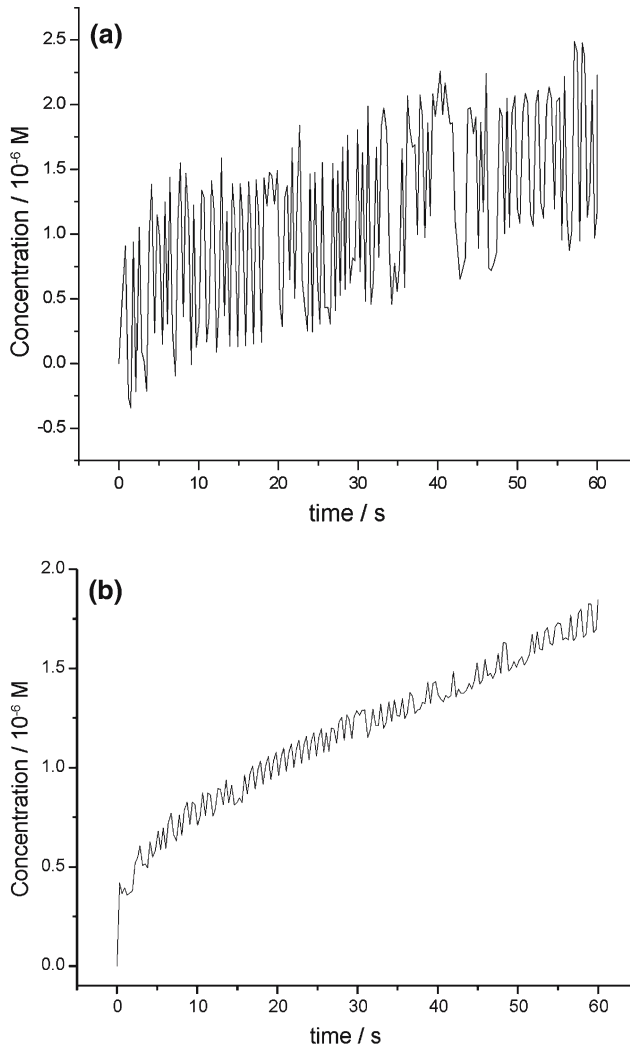


Figure 4. Concentration distribution of NO₃ computed using (a) the AP method, and (b) the ARK method with tolerance $\varepsilon = 10^{-6}$.

As can be seen from table 3 the CPU time is much higher in the case of the AP method whereas the number of steps for this method is significantly smaller than that for the ARK method. This example emphasizes that the AP method becomes increasingly inefficient as the dimensionality of the problem increases. The increased number of arithmetic operations results also in increased round-off errors which is reflected in lower convergence rate as exemplified in figures 3 and 6.

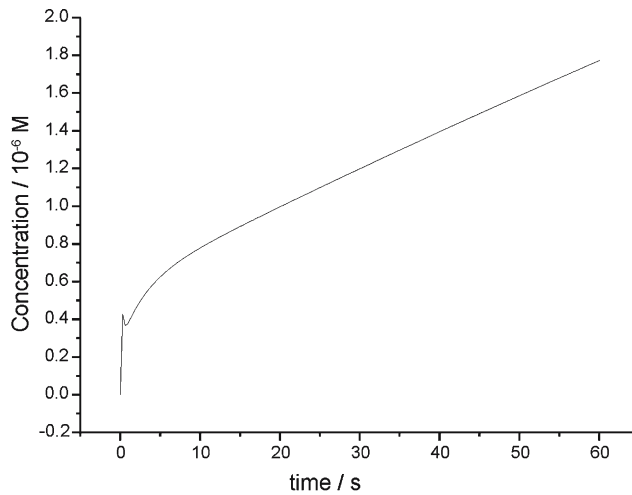
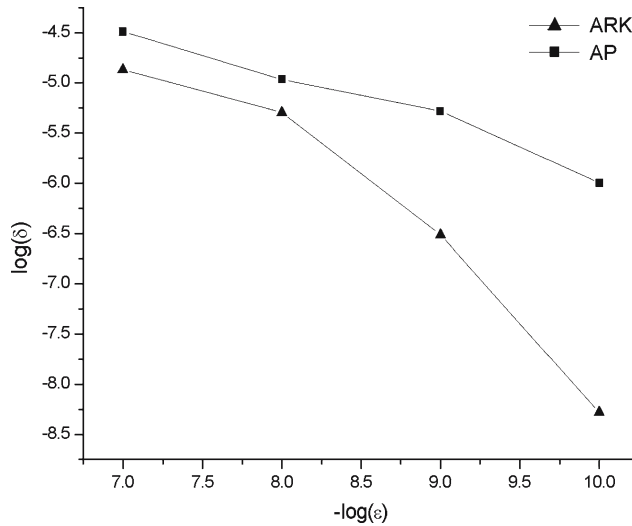
Figure 5. Converged concentration distribution of NO_3 .

Figure 6. Log-log plot of maximum relative error in computed concentrations as a function of tolerance for the ARK and AP methods (pollution problem).

4. Conclusions

The comparison of the ARK and AP methods revealed that both methods are capable of solving large and extremely stiff ODE systems. Nevertheless the ARK method is superior to the AP method in terms of computational costs and convergence rate, especially for large ODE systems, despite the fact that it requires smaller integration steps.

5. Acknowledgments

O.V. Klymenko and I.B. Svir wish to thank NATO for the Reintegration Grant (NUKR.RIG 981488).

References

- [1] O.V. Klymenko and I.B. Svir, Management information: systems and devices. All-Ukr. Sci. Interdep. Mag. 121 (2002) 30.
- [2] O.V. Klymenko, Radioelektronika i informatika 3 (2004) 42.
- [3] G. Hall and J.M. Watt (eds.), *Modern Numerical Methods for Ordinary Differential Equations* (Clarendon Press, Oxford, UK, 1976).
- [4] A.A. Samarskii and A.V. Gulin, *Numerical Methods* (Nauka, Moscow, 1989).
- [5] L. Collatz, *Numerical Treatment of Differential Equations* (Springer, Berlin, 1966).
- [6] C.W. Gear, *Numerical Initial Value Problem in Ordinary Differential Equations* (Prentice-Hall, Englewood Cliffs, NJ, 1971).
- [7] J.C. Butcher and N. Rattenbury, Appl. Numer. Math. 53 (2004) 165.
- [8] C. Aluffi-Pentini, V. De Fonzo and V. Parisi, J. Math. Chem. 33 (2003) 1.
- [9] J.C. Butcher, Appl. Numer. Math. 24 (1997) 331.
- [10] V.N. Shulyk, O.V. Klymenko and I.B. Svir, Radioelektronika i informatika 3 (2005) 28.
- [11] A.M. Zhabotinskii, Biofizika, 9 (1964) 306.
- [12] E. Hairer, S.P. Nørsett and G. Vanner, *Solution of Ordinary Differential Equations. Non-stiff Problems* (Mir, Moscow, 1990).
- [13] I.B. Svir, O.V. Klymenko, A.I. Oleinick and M.S. Platz, Radioelektronika i informatika 4 (2004) 21.
- [14] W.M. Lioen and J.J.B. de Swart, Test Set for Initial Value Problem Solvers. <http://www.cwi.nl/cwi/projects/IVPtestset/>.
- [15] J.G. Verwer, SIAM J. Sci. Comput. 15 (1994) 1243.